

GROWTH AND INVESTIGATION OF $\text{La}_{1-x}\text{R}_x\text{MnO}_3$ ($R = \text{Ba, Ca, Ce}$) THIN FILMS

R. Butkutė^a, J. Devenson^a, M.A. Rosa^b, M. Godinho^b, A.K. Oginskis^a,
F. Anisimovas^a, A. Vailionis^c, and B. Vengalis^a

^a Semiconductor Physics Institute, A. Goštauto 11, LT-01108 Vilnius, Lithuania
E-mail: renata@pfi.lt

^b Department of Physics, University of Lisbon, Ed C8, 1749-016 Lisbon, Portugal

^c Geballe Laboratory for Advanced Materials, Stanford University, 476 Lomita Mall, CA 94305-4045 Stanford, USA

Received 15 November 2005

Thin $\text{La}_{1-x}\text{R}_x\text{MnO}_3$ ($R = \text{Ba, Ca, Ce}$) films ($d = 40\text{--}400$ nm) were grown on single crystal NdGaO_3 (100), SrTiO_3 (100), LaAlO_3 (100), and MgO substrates using magnetron sputtering and pulsed laser deposition techniques. X-ray diffraction patterns (XRD) revealed high crystalline quality of the $\text{La}_{2/3}\text{Ca}_{1/3}\text{MnO}_3$ and $\text{La}_{2/3}\text{Ba}_{1/3}\text{MnO}_3$ films grown on lattice-matched SrTiO_3 , LaAlO_3 , and NdGaO_3 . Meanwhile, weak reflexes in $\Theta\text{--}2\Theta$ scans demonstrating traces of CeO_2 impurities have been indicated for the $\text{La}_{2/3}\text{Ce}_{1/3}\text{MnO}_3$ films. Series of post-deposition annealing experiments demonstrated a crucial role of annealing temperature and ambience on both electrical and magnetic properties of the $\text{La}_{2/3}\text{Ce}_{1/3}\text{MnO}_3$ films.

Keywords: manganites, thin film magnetic and electrical properties, colossal magnetoresistance

PACS: 75.47.Lx, 75.70.Ak, 75.47.De

1. Introduction

Perovskite manganites referred to as $\text{La}_{1-x}\text{R}_x\text{MnO}_3$ ($R = \text{Ca, Sr, Ba, Pb, etc.}$) exhibit a rich variety of electronic and magnetic properties due to a strong coupling between spin, charge, and orbital degrees of freedom [1–5]. The parent compound, LaMnO_3 , is an anti-ferromagnetic insulator, whereas the doped materials, $\text{La}_{1-x}\text{R}_x\text{MnO}_3$ with $x \cong 0.33$ are ferromagnetic metals demonstrating a metal–insulator transition at a Curie temperature (T_c) depending on x .

Hole doping is achieved in these compounds by substituting a bivalent cation such as Ca, Ba, or Sr at a rare earth site. The hole-doped compounds show large negative magnetoresistance close to the ferromagnetic transition temperature T_c . This feature is explained within a model based on a double exchange interaction through e_g electrons: a proportionate amount of Mn^{3+} with electronic configuration $t_{2g}^3 e_g^1$ is substituted with Mn^{4+} giving holes in the e_g band [6].

La–Ce–Mn–O is unique in this family since trivalent La is partially replaced by a tetravalent Ce instead of bivalent Ca, Sr, and Ba ions. In this case, a mixed-valence ($\text{Mn}^{3+} - \text{Mn}^{2+}$) state is expected, and thus one could expect appearance of electron doping

on the manganese site [7–8]. Such electron-doped system could be very promising for fabrication of $p\text{--}n$ homojunctions in novel spintronics devices. Unfortunately, up to now Ce-doped manganites are not well examined compared to similar hole-doped systems. Mandal and Das [7] pointed out electron doping of bulk $\text{La}_{1-x}\text{Ce}_x\text{MnO}_3$ ceramic; however, hole-like behaviour has been certified recently for the material from thermopower data [9]. Later it was found that Ce-doped material may be characterized by a hole-doped lanthanum-deficient phase with cerium oxide as an impurity phase [10]. Difficulties in doping of manganite films by Ce and presence of peaks in the X-ray diffraction spectra corresponding to CeO_2 impurities were also reported [11, 12]. Meanwhile, in [13–15] it was demonstrated that it is possible to fabricate single-phase Ce-doped manganite films using pulsed laser deposition.

In this paper we report a systematic investigation of structural, electrical, and magnetic properties of $\text{La}_{1-x}\text{R}_x\text{MnO}_3$ (with $x = 0.33$ and $R = \text{Ca, Ba, Ce}$) films grown on different substrates by applying two deposition techniques, i. e. pulsed laser deposition (PLD) and dc magnetron sputtering (MS). The aim of this work was to optimize deposition conditions of the mangan-

ite films to be used for fabrication of various device structures. Since physical properties of the manganites depend strongly on microstructure and oxygen content, the effects of post-annealing under oxidation and reduction atmospheres on electrical and magnetic properties as well as on the surface quality were examined.

2. Experimental details

Disk-shaped ceramic targets with stoichiometric $\text{La}_{2/3}(\text{Ca}, \text{Ba}, \text{Ce})_{1/3}\text{MnO}_3$ compositions were used for pulsed laser ablation and dc magnetron sputtering. The targets were prepared by a conventional solid state reaction using high purity powdered La_2O_3 , CaCO_3 , BaCO_3 , CeO_2 , and Mn_2O_3 . After being mixed, the powders were heated in air at 950°C for 20 h followed by an intermediate grinding for homogenization, pelletizing, and final sintering at 1150°C for 20 h.

Thin manganite films were deposited on lattice matched single-crystal SrTiO_3 (100) (lattice parameter $a_0 = 0.3905$ nm), LaAlO_3 (100) ($a_0 = 0.3820$ nm), NdGaO_3 (100) ($a_0 = 0.3880$ nm), as well as MgO (100) ($a_0 = 0.4203$ nm, lattice mismatch $\sim 8\%$) and lucalox (polycrystalline Al_2O_3). During film growth, temperature of the substrate was held fixed ($T = 650$ – 750°C), and gas pressure was kept at about 15 and 25 Pa for MS and PLD, respectively. In order to find the optimum gas mixture, several $\text{Ar}:\text{O}_2$ ratios (0.25:0.75, 0.5:0.5, and 0.75:0.25) were used for MS deposition, whereas oxygen pressure was kept constant for PLD. In both cases after film deposition, the growth chamber was vented with pure oxygen (1 atm.) and the films were cooled down slowly to a room temperature. The films were post-annealed at temperatures ranging from 450°C to 850°C either in a flowing O_2 or Ar gas or under low vacuum (10^{-5} Torr) conditions. Thickness of the films ranged from 40 to 400 nm.

Crystalline structure of the prepared films was examined by high resolution XRD measurements using monochromatic $\text{Cu K}\alpha$ radiation. Electrical resistance measurements were performed in a wide temperature range (78–330 K) using a standard four-point probe configuration and applying direct current of about 10 μA . Magnetoresistance of the films (MR) was measured by applying a magnetic field of 1 T.

3. Results and discussion

High crystalline quality of $\text{La}_{2/3}\text{Ca}_{1/3}\text{MnO}_3$ and $\text{La}_{2/3}\text{Ba}_{1/3}\text{MnO}_3$ thin films deposited on lattice

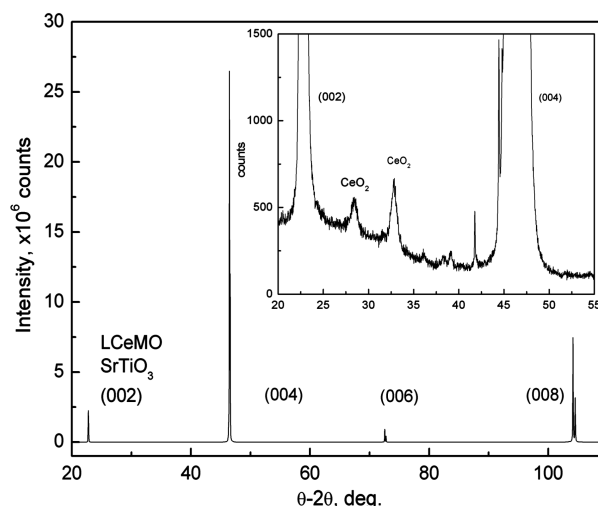


Fig. 1. X-ray Θ – 2Θ patterns measured for $\text{La}_{0.67}\text{Ce}_{0.33}\text{MnO}_3$ thin film grown on SrTiO_3 (100) substrate. Inset presents an enlarged view of XRD scan demonstrating weak reflexes of CeO_2 .

matched SrTiO_3 , LaAlO_3 , and NdGaO_3 substrates either by MS or PLD has been certified by measuring their Θ – 2Θ X-ray diffraction spectra. Clearly defined reflection peaks from the planes of (00 l) family were observed in Θ – 2Θ spectra of the films. Similar XRD patterns have been measured for the $\text{La}_{2/3}\text{Ce}_{1/3}\text{MnO}_3$ films (see Fig. 1) although weak reflexes seen at about 28° and 33° have demonstrated presence of a negligible amount of CeO_2 phase (see inset to Fig. 1). At the same time, polycrystalline quality has been indicated from XRD measurements for the $\text{La}_{2/3}\text{Ca}_{1/3}\text{MnO}_3$, $\text{La}_{2/3}\text{Ba}_{1/3}\text{MnO}_3$, and $\text{La}_{2/3}\text{Ce}_{1/3}\text{MnO}_3$ films grown on mismatched MgO (100) substrate and lucalox.

Figure 2(a) presents the resistance R versus T plots for high crystalline quality Ca, Ba, and Ce-doped films grown on lattice-matched SrTiO_3 (100) substrates. The characteristic resistance peaks corresponding to the transition from a paramagnetic insulating (PI) to a ferromagnetic metallic (FMM) phase (at $B = 0$ T) were observed at 250, 285, and 270 K, for the $\text{La}_{2/3}\text{Ca}_{1/3}\text{MnO}_3$, $\text{La}_{2/3}\text{Ba}_{1/3}\text{MnO}_3$, and $\text{La}_{2/3}\text{Ce}_{1/3}\text{MnO}_3$ films, respectively. The curves presented in Fig. 2(b) demonstrate temperature-dependent magnetoresistance for the same films at $B = 1$ T. It is worth noting a relatively sharp resistance drop seen for the $\text{La}_{2/3}\text{Ce}_{1/3}\text{MnO}_3$ film while similar resistive transitions for the $\text{La}_{2/3}\text{Ca}_{1/3}\text{MnO}_3$ and $\text{La}_{2/3}\text{Ba}_{1/3}\text{MnO}_3$ films were indicated in a significantly wider temperature range.

Shift of T_c values down to (150–180) K and broadening of the resistive PI–FMM transition were indicated for the $\text{La}_{2/3}\text{Ca}_{1/3}\text{MnO}_3$ films with their annealing in vacuum. However, subsequent saturation of these samples by oxygen at 550°C caused a reversible increase

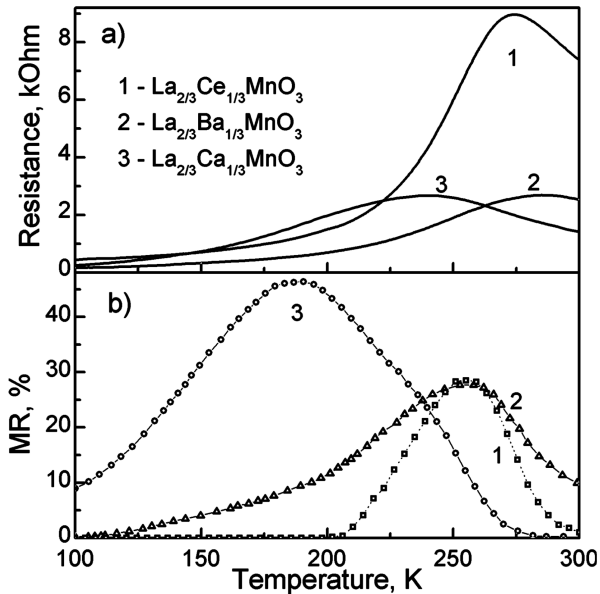


Fig. 2. (a) Resistance versus temperature of as-grown 400 nm thick $\text{La}_{2/3}\text{Ca}_{1/3}\text{MnO}_3$, $\text{La}_{2/3}\text{Ba}_{1/3}\text{MnO}_3$, and $\text{La}_{2/3}\text{Ce}_{1/3}\text{MnO}_3$ films deposited on NdGaO_3 (100) substrate. (b) Magnetoresistance of the $\text{La}_{2/3}\text{Ca}_{1/3}\text{MnO}_3$, $\text{La}_{2/3}\text{Ba}_{1/3}\text{MnO}_3$, and $\text{La}_{2/3}\text{Ce}_{1/3}\text{MnO}_3$ films at $B = 1$ T as a function of temperature.

of T_c and a significant sharpening of their resistive PI–FMM transition. In the case of $\text{La}_{2/3}\text{Ba}_{1/3}\text{MnO}_3$ films, the annealing ambience had negligible influence on T_c value, although annealing of the samples at higher temperatures (500–550 °C) resulted in sharper resistive transition. Thus, one can conclude that oxygen is introduced into the $\text{La}_{2/3}\text{Ca}_{1/3}\text{MnO}_3$ and $\text{La}_{2/3}\text{Ba}_{1/3}\text{MnO}_3$ lattice more homogeneously during annealing at high temperatures.

Post-annealing of the $\text{La}_{2/3}\text{Ce}_{1/3}\text{MnO}_3$ films, unlike that of $\text{La}_{2/3}\text{Ca}_{1/3}\text{MnO}_3$ and $\text{La}_{2/3}\text{Ba}_{1/3}\text{MnO}_3$ films, caused significant irreversible changes in their resistance–temperature dependence. Figure 3 shows the resistance versus temperature plots displayed for the $\text{La}_{2/3}\text{Ce}_{1/3}\text{MnO}_3$ film ($d = 400$ nm) measured just after deposition (curve 1), after annealing in vacuum (curve 2) and after the subsequent annealing in oxygen ambient ($p_{\text{O}_2} = 10^5$ Pa) at 550 °C (curve 3). It can be seen from the figure that annealing of the films in vacuum causes significant resistance increase and a shift of the resistance anomaly (related to the PM–FM transition) to the lower temperatures. Meanwhile, additional annealing of the film in oxygen results only in a slight shift of the resistance anomaly to higher temperature side and a sharp resistance decrease with T decreasing below 125 K. Both the $R(T)$ anomaly at 200 K and the resistance drop below 125 K demonstrate the phase separation phenomenon, i.e. the coexistence of two phases characterized by two phase

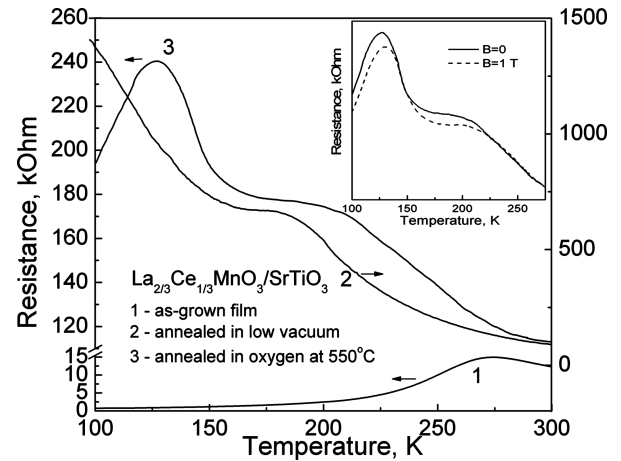


Fig. 3. Effect of post-annealing conditions on temperature-dependent resistance of $\text{La}_{2/3}\text{Ce}_{1/3}\text{MnO}_3$ films grown on NdGaO_3 (100) substrate. The insert shows the resistance versus temperature at external magnetic field $B = 0$ and 1 T measured for the film annealed under low vacuum conditions followed by annealing in oxygen atmosphere.

transition temperatures (T_{c1} and T_{c2}). Additional evidence supporting the phase separation phenomenon in $\text{La}_{2/3}\text{Ce}_{1/3}\text{MnO}_3$ film has been obtained from R versus T measurements under applied magnetic field (see inset to Fig. 3 demonstrating significant magnetoresistance of the films in the vicinity of T_{c1} and T_{c2}). In our opinion, the phase separation phenomenon observed for the annealed $\text{La}_{2/3}\text{Ce}_{1/3}\text{MnO}_3$ film demonstrates instability of Ce-doped state with respect to the appearance of cation-deficient material during long-term annealing. We believe that the observed resistance drop below 125 K may be associated with intergrain boundaries while the resistance anomaly in the vicinity of T_{c2} demonstrates cation deficient material of grains.

The study of substrate influence on electrical and magnetic properties of the manganite films has revealed that all the films grown on lattice-matched SrTiO_3 (100), LaAlO_3 (100), and NdGaO_3 (100) reach their maximum T_c values characteristic of high quality $\text{La}_{2/3}\text{Ca}_{1/3}\text{MnO}_3$, $\text{La}_{2/3}\text{Ba}_{1/3}\text{MnO}_3$, and $\text{La}_{2/3}\text{Ce}_{1/3}\text{MnO}_3$ thin films reported earlier by various authors. The films grown on MgO substrates and lucalox were polycrystalline. They all exhibited higher values of room temperature resistance and significantly lower T_c values (from 100 K to 150 K) compared to similar films on lattice-matched perovskite substrates (see Fig. 4, curves 1 and 3).

Furthermore, the effect of film thickness on electrical and magnetic properties was investigated for the $\text{La}_{2/3}\text{Ca}_{1/3}\text{MnO}_3$, $\text{La}_{2/3}\text{Ba}_{1/3}\text{MnO}_3$, and $\text{La}_{2/3}\text{Ce}_{1/3}\text{MnO}_3$ films grown on lattice matched SrTiO_3 (100), LaAlO_3 (100), and NdGaO_3 (100) sub-

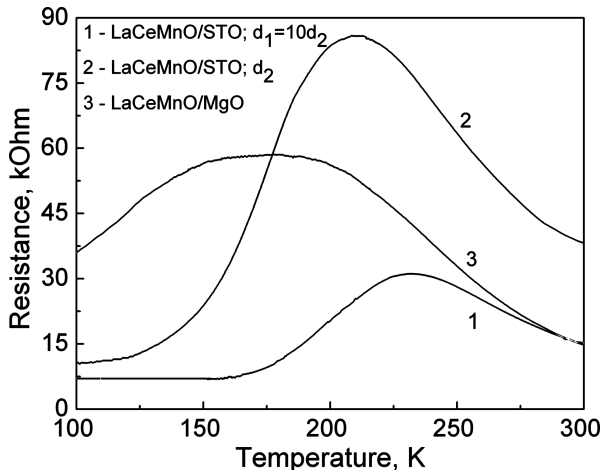


Fig. 4. Influence of film thickness and substrate lattice parameter on temperature dependence of resistance of $\text{La}_{2/3}\text{Ce}_{1/3}\text{MnO}_3$ films. Curves 1 and 2 demonstrate the R - T behaviours of 400 nm and 40 nm thick films deposited on lattice-matched SrTiO_3 (100); curve 3 was measured for 400 nm thick $\text{La}_{2/3}\text{Ce}_{1/3}\text{MnO}_3$ film deposited on MgO substrate (lattice mismatch $\sim 8\%$).

strates. In Fig. 4 we present typical R versus T dependences for epitaxial $\text{La}_{2/3}\text{Ce}_{1/3}\text{MnO}_3$ films grown on SrTiO_3 (100) of different thicknesses (curves 1 and 2). It is seen that T_c slightly decreases with decreasing thickness. Similar thickness dependent T_c was found for $\text{La}_{2/3}\text{Ca}_{1/3}\text{MnO}_3$ and $\text{La}_{2/3}\text{Ba}_{1/3}\text{MnO}_3$ films deposited on SrTiO_3 (100), LaAlO_3 (100), and NdGaO_3 (100) substrates.

4. Summary

We report electrical and magnetic properties of the $\text{La}_{2/3}\text{Ca}_{1/3}\text{MnO}_3$, $\text{La}_{2/3}\text{Ba}_{1/3}\text{MnO}_3$, and $\text{La}_{2/3}\text{Ce}_{1/3}\text{MnO}_3$ films laser deposited and magnetron sputtered on different substrates. Both X-ray diffraction and transport measurements revealed the growth of single crystal and single phase $\text{La}_{2/3}\text{Ca}_{1/3}\text{MnO}_3$ and $\text{La}_{2/3}\text{Ba}_{1/3}\text{MnO}_3$ films on lattice-matched SrTiO_3 (100), LaAlO_3 (100), and NdGaO_3 (100) substrates. These films showed a metal–insulator transition at 250 K and 285 K. However, additional XRD peaks of CeO_2 (less than 1%) have been indicated in XRD spectra of $\text{La}_{2/3}\text{Ce}_{1/3}\text{MnO}_3$ layers. Irreversible decrease of both the T_c values and the relative volume of the ferromagnetic $\text{La}_{2/3}\text{Ce}_{1/3}\text{MnO}_3$ phase with additional annealing of the films at $T \geq 550^\circ\text{C}$ demonstrate thermal instability of the doped material in respect to appearance of nonstoichiometry in the cation subsystem.

The growth of manganites on lattice-matched substrates enabled one to achieve the highest T_c values re-

ported up to now for the best quality $\text{La}_{2/3}\text{Ca}_{1/3}\text{MnO}_3$, $\text{La}_{2/3}\text{Ba}_{1/3}\text{MnO}_3$, and $\text{La}_{2/3}\text{Ce}_{1/3}\text{MnO}_3$ thin films. Meanwhile, the polycrystalline films exhibited enhanced room temperature resistance and lower T_c values. T_c of all the films slightly decreased with thickness decreasing from 400 nm down to 40 nm.

Acknowledgements

This work has been supported partially by EC project PRAMA, tract Nr. G5MA-CT-2002-04014FP-5 and the Swedish government Visby programme grant.

References

- [1] S. Jin, T.H. Tiefel, M. McCormark, R.A. Fastnacht, R. Ramesh, and L.H. Chen, *Science* **264**, 413 (1994).
- [2] J. Fontcuberta, B. Martinez, A. Seffer, S. Pinol, J.L. Garcia-Munoz, and X. Obaradors, *Phys. Rev. Lett.* **76**, 1122 (1996).
- [3] J.-Q. Wang, R.C. Barker, G.-J. Cui, T. Tamagawa, and B.L. Halpern, *Appl. Phys. Lett.* **71**, 3418 (1997).
- [4] Y. Lu, X.W. Li, G.Q. Gong, G. Xiao, A. Gupta, P. Leoeur, J.Z. Sun, Y.Y. Wang, and V.P. Dravid, *Phys. Rev. B* **54**, R8357 (1996).
- [5] J.Z. Sun, W.J. Gallagher, P.R. Duncombe, L. Krusin-Elbaum, R.A. Altman, A. Gupta, Y. Lu, G.Q. Gong, and G. Xiao, *Appl. Phys. Lett.* **69**, 3266 (1996).
- [6] C. Zener, *Phys. Rev.* **82**, 403 (1951).
- [7] P. Mandal and S. Das, *Phys. Rev. B* **56**, 15073 (1997).
- [8] C. Mitra, P. Raychaudhuri, G. Kobernik, K. Dorr, K.H. Muller, L. Schultz, and R. Pinto, *Appl. Phys. Lett.* **79**, 2408 (2001).
- [9] J. Philips and T.R.N. Kutty, *J. Phys.: Condensed Matter* **11**, 8537 (1999).
- [10] R. Ganguly, I.K. Gopalakrishnan, and J.V. Yakhmi, *J. Phys.: Condensed Matter* **12**, L719 (2000).
- [11] Y.G. Zhao, R.C. Srivastava, P. Fournier, V. Smolyaninova, M. Rajeswari, T. Wu, Z.Y. Li, R.L. Greene, and T. Venkatesan, *J. Magn. Magn. Mater.* **220**, 161 (2000).
- [12] V.L. Joseph Joly, P.A. Joy, and S.K. Date, *J. Magn. Magn. Mater.* **247**, 316 (2002).
- [13] C. Mitra, P. Raychaudhuri, J. John, S.K. Dhar, A.K. Nigam, and R. Pinto, *J. Appl. Phys.* **89**, 524 (2001).
- [14] P. Raychaudhuri, S. Mukherjee, A.K. Nigam, J. John, U.D. Vaisnav, R. Pinto, and P. Mandal, *J. Appl. Phys.* **86**, 5718 (1999).
- [15] C. Mitra, Z. Hu, P. Raychaudhuri, S. Wirth, S.I. Csiszar, H.H. Hsieh, H.-J. Lin, C.T. Chen, and L.H. Tjeng, *Phys. Rev. B* **67**, 092404 (2003).

La_{1-x}R_xMnO₃ (R – Ba, Ca, Ce) PLONŲJŲ SLUOKSNIŲ AUGINIMAS IR TYRIMAS

R. Butkutė^a, J. Devenson^a, M.A. Rosa^b, M. Godinho^b, A.K. Oginskis^a, F. Anisimovas^a, A. Vailionis^c,
B. Vengalis^a

^a *Puslaidininkų fizikos institutas, Vilnius, Lietuva*

^b *Lisabonos universitetas, Lisabona, Portugalija*

^c *Stenfordo universitetas, Stenfordas, JAV*

Santrauka

Ploni La_{1-x}R_xMnO₃ (čia $x = 0,33$, o $R = \text{Ba, Ca arba Ce}$) sluoksniai ($d = 40\text{--}400$ nm) buvo pagaminti magnetroninio dulkinimo ir lazerinio garinimo būdais ant monokristalinių LaAlO₃, NdGaO₃, SrTiO₃ padėklų, kristalinio MgO ir polikoro naudojant tos pačios cheminės sudėties keraminius taikinius. La_{2/3}(Ba, Ca, Ce)_{1/3}MnO₃ sluoksniai, užauginti ant suderintų gardelių LaAlO₃, NdGaO₃ ir SrTiO₃ padėklų, pasižymėjo aukštomis virsmo iš paramagnetinės į feromagnetinę būseną temperatūromis T_c (atitinkamai 285, 250 ir 270 K), o jų didžiausios magnetovaržos

vertės, esant $B = 1$ T, kito nuo 25 iki 48%. Tuo tarpu tokių pačių polikristalinių sluoksnių, užaugintų ant MgO ir polikoro, Kiuri temperatūros vertės buvo mažesnės (100–150 K). Tiriant deguonies kiekio įtaką bandinių krizinei temperatūrai bei magnetovaržai, paaiškėjo, kad papildomai pakaitinus LaCaMnO ir LaBaMnO sluoksnius aukštoje (550 °C) temperatūroje, jų T_c vertės būna šiek tiek mažesnės, o elektrinės varžos kitimas ties Kiuri temperatūra – staigesnis. Be to, nustatyta, jog pageidaujama LaCaMnO virsmo temperatūros vertę galima pasiekti, pasirinkus atkaitinimo aplinką (deguonį arba vakuumą).